

A New Methodology for Efficiency Scaling of Pumps-as-Turbines (PATs) and Its Application to two South Africa 13kW and 100kW Micro Hydropower Systems

Ricardo N. Van Zeller
ricardo.van.zeller@tecnico.ulisboa.pt

Instituto Superior Técnico, Universidade de Lisboa, Portugal

May 2020

Abstract

Hydropower is the most mature renewable energy resource in the world. Not only it represents a large portion of the renewable energy generated in the world, as it is estimated that most of its potential is yet to be explored, with the biggest focus on micro and small hydropower systems. However, the cost-effectiveness of these systems still needs to improve, with pump-as-turbines (PATs) playing a key role on the reduction of the investment costs. The drawback of these types of turbomachines relies on the fact that pump manufacturers do not provide, nor test, the operating condition of a pump working as a turbine. In this thesis, it was developed a new methodology to predict the efficiency curves of a reverse-running centrifugal pump. This numerical method is based on a theory developed by Gülich to predict the efficiency curves of a centrifugal pump taking into account the influence of the roughness and Reynolds number on the efficiency scaling. Later, the numerical method was implemented in Microsoft Excel in order to create the Scaling of PAT Efficiency Curves program, or SPATEC. In addition, the numerical model was applied to an extensive number of cases that correlate different PATs found in literature. As a consequence, the absolute and relative error ranges were successfully ascertained for both the flow rate and head efficiency curves. Finally, the same model was applied to two real-life cases of micro hydropower systems and the precision of the efficiency prediction assessed.

Keywords: Hydropower, energy saving, PAT, efficiency prediction, similarity laws

1. Introduction

To combat the increasing demand of electricity, researchers are seeking for improved techniques to overcome some relevant issues associated with power generation. One of the most suitable solutions is thought to be renewable energy, specially hydropower.[1] In many developing countries, specially within the Sahara African region, small and micro hydropower systems represent a valuable solution to generate electricity. An energetically efficient solution relies on the idea of pumps working as turbines (also known as pump-as-turbines or PATs). Whenever reverse-runned, pumps can generate and recover power in small and micro hydropower schemes with very satisfying efficiencies. Their simple layout, accessible purchase cost and “off-the-shelf” worldwide readiness are some advantages of these PATs, which naturally promotes their choice over hydraulic turbines. At an economic point of view, reverse-running pumps were found to have a capital payback period lower than 2 years, for capacities varying between 5 kW and

50 kW,[2, 3].

However, there is still a significant drawback: predicting the actual PAT performance for a specific point of operation, specially the best efficiency point (BEP). This problem arises from the fact that pump manufactures do not provide, nor test, any pump characteristics in turbine-mode.

In this thesis, it is presented an alternative methodology to predict PAT performance curves. Based on turbine-mode operating points of several pumps, the efficiency curves of a particularly intended PAT might be achieved (for a specific speed between 0.12 and 1.18). This work is based on a methodology developed by [7] to predict efficiency curves for geometrically similar centrifugal pumps, taking into account the influence that the roughness and the Reynolds number have on the performance.

2. Background

A pump-as-turbine (PATs) is a pump that runs with the impeller and the flow in an opposite direc-

tion to that defined for the pump operation mode.

On the contrary to conventional turbines, PATs do not exhibit any type of regulation, which is a natural consequence of running a pump in its opposite direction. Additionally, PATs have a larger runner, with the blades' curvature in an opposite direction as well. Despite the extra cost associated with a larger runner and the small efficiency loss inherent to the unregulated operation mode, PATs are still cost-effective due to its mass production.

To avoid the decelerated flow issues normally associated with pumps, the pump's impeller must be bigger (30% to 40% bigger) than the one of a turbine, with long and gradually diverging channels. In addition, reversed curvatures and small angles at the tip of the blades are also some geometrical characteristics that must be adopted to increase the stability of the flow.

In the opinion of some researchers [13, 4], an immediately available PAT, that does not need to be specially manufactured to suit particular specifications, can be found with maximum power of 100 kW and 250 kW. However, there are a few countries, like Nepal and Pakistan that hardly own PATs with capacities superior to 15 kW, for relatively low specific speeds.

Apart from power, PATs might also be limited according to their specific speed, Ω . The specific speed is a non-dimensional parameter of turbomachines used to understand which flow properties (namely, flow rate Q and head H) are accepted to circulate through the machine with a particular rotational speed. Low specific speeds are associated with a high head potential and a low flow rate, whilst a low head and a high flow rate induce high specific speeds.

In a general way, it is not possible to ascertain a particular range to define lower and upper specific speed limits of applicability of PATs. When it comes to lower specific speeds, some authors like [15] defend that PATs cannot compete with Pelton turbines for $\Omega \leq 0.2$, whilst others ([6, 8, 9, 14] state that multistage PATs can still be a cost-effective solution in countries where the cost of manufacturing is competitive enough against impulse turbines.

On the other hand, high specific speed PATs (described by their axial flows) have disadvantages like higher cost, lack of experimental information when operating in turbine-mode [16], and blade shape impairments on the stability of the flow once it was designed to operate in pump-mode, [10]. Besides, they have a bias towards cavitation and low efficiencies so that, high specific speed axial-flow or mixed-flow PATs might be the most suitable PAT types to install in low head hydropower sites, that represent most of the small hydro potential in the world [11].

3. Dimensionless coefficients and similarity laws

In a pump with incompressible flow there are different types of variables that characterize its operation, such as control variables, fluid properties and geometric variables. The control variables consist in parameters that are deliberately altered to regulate the operation of the turbomachinery. As for the properties of the fluid, it is easily noticed that properties such as the specific mass and the viscosity considerably affect the operating characteristics of the turbomachine. Finally, when it comes to geometric variables, changing the turbomachine implies a naturally different functioning of the system: its operation not only depends on the absolute dimensions of the machine (for example, the outlet impeller diameter), but also on a large number of angles and dimensionless relations α, β , etc.

The mathematical theorem, known as Buckingham's theorem, along with the control variables, the fluid's properties and the geometric variables that characterize a turbomachine, allow the determination of the remaining variables of the system, which are dependent of the former parameters. For some of these variables it might be useful to disregard or assume certain dimensionless parameters as constant and also to disregard the so known Reynolds number.

Any dependent variable can be defined as a function of dimensionless parameters, which means that they do not depend on the unit system considered, as long as it remains consistent. These dimensionless variables allow the characterization of a single curve for a family of geometrically similar turbomachines, instead of representing a curve for each turbomachine considered. This happens because geometrically similar pumps imply similar dimensionless coefficients [5].

In addition, the exchange between dimensionalized and non-dimensionalized curves is rather straightforward: both the transformation from the dimensionless curve to the dimensional curve, and vice-versa, only requires the knowledge of two characteristics of the pump's operation apart from the flow rate and head, for example, the diameter and the rotation speed. This might be useful for anyone that works with a unit system different from the one with which the pump operating curves are drawn. The exchange between dimensional curves is also possible without incurring to the dimensionless representation of the pump curve. The solution simply consists in equalizing the dimensionless coefficients of both curves and is useful to modify a certain pump characteristics.

Apart from changing between dimensional curves for a certain pump, non-dimensional coefficients also allow the exchange of operating curves between a family of geometrically similar pumps,

even if they have distinct absolute dimensions. The resulting equations are known as similarity or affinity laws. Equations 1 to 5 present the most usual non-dimensional correlations.

$$\eta_B = \eta_A \quad (1)$$

$$\Omega_B = \Omega_A \quad (2)$$

$$\frac{Q_B}{Q_A} = \frac{N_B}{N_A} \left(\frac{D_{2B}}{D_{2A}} \right)^3 \quad (3)$$

$$\frac{H_B}{H_A} = \left(\frac{N_B}{N_A} \right)^2 \left(\frac{D_{2B}}{D_{2A}} \right)^2 \quad (4)$$

$$\frac{P_B}{P_A} = \frac{\rho_B}{\rho_A} \left(\frac{D_{2B}}{D_{2A}} \right)^5 \left(\frac{N_B}{N_A} \right)^3, \quad (5)$$

with subscripts "A" and "B" representing two distinct points of operation.

The fact that geometrically similar turbomachines imply similar dimensionless operating curves, allows the estimation of the dimensionless curve of a reduced model to perceive the behavior of the respective prototype in the conditions of the system that is intended to design. However, it is important to realize that, due to the neglect of factors like the Reynolds number and geometric scaling effects, the working curve of the prototype will present different results from those verified in reality. The scale effects result from the natural impossibility of the prototype to obtain a geometry perfectly similar to that of the model. For example, the relative roughness and axial clearances between the rotor and the stator are absolute dimensions that change depending on the size of the turbomachine.

From all dimensionless parameters, the most frequently used to correlate geometrically similar pumps is the specific speed Ω . The specific speed is also a characteristic parameter of turbomachines: it defines the geometry with which a machine must be designed.

4. Power Balance and Efficiencies

Whenever operating with a turbomachine, there are losses associated with the process of machining. According to [7], these losses are dissipated into heat and, after some rearrangement, can be divided into three major groups: mechanical losses P_{mec} , volumetric losses P_{vol} , hydraulic losses P_{hyd} .

Inside a centrifugal pump, mechanical losses are due to the friction forces exerted on the radial bearings, axial bearing and shaft seals. The volumetric losses consist of leakages through several components of the pump that result in kinetic energy losses and, consequently, head and efficiency reductions. Any friction or vortex dissipation of energy that takes place between the suction and dis-

charge nozzle is defined as a hydraulic loss. Skin friction losses are a consequence from the shear stresses created between the fluid and the boundary layer of a body. These losses are highly dependent on the roughness ε , not so much on the Reynolds number Re and, unlike vortex losses, they have more importance in thin boundary layers and attached flows. As for vortex dissipations, also known as mixing losses, they constitute another important set of losses, within the hydraulic losses - the mixing losses, that constitutes a major part of the total losses, particularly for high specific speeds. These losses are caused by turbulent dissipation that occurs when the streamlines exchange momentum between themselves.

5. Materials and Methods

5.1. New methodology for PAT efficiency scaling

The methodology used to calculate the efficiency and characteristics of a centrifugal pump working as a turbine (PAT) takes as reference the efficiency and characteristics of a geometrically similar pump (i.e. with the same specific speed). The pump, whose characteristics needed to be determined, was defined as the prototype (subscript "p"), whilst the reference pump is known as the model (subscript "M").

The implementation of such procedure provides an understanding of the impact that the Reynolds number, roughness and specific speed have on the different types of losses and, subsequently, on the efficiency of a PAT. Additionally, this method can also be used in any type of flow conditions and surface roughnesses and still provide stable results.

Hydroelectric projects are one of the many cases where efficiency scaling is applied. Herein, the real site flow conditions and the planned infrastructure (prototype) are reproduced in a small scale with the best possible precision (model) and tested in a laboratory to understand and evaluate the real project prior to its implementation. For that, it is mandatory to know several model and prototype characteristics, see Table 1.

Model, M		Prototype, p	
N_M	Rotational speed	N_p	Rotational speed
Q_M	Flow rate at the BEP	P_p	Total power
H_M	Head at the BEP	ν_p	Kinematic viscosity
D_M	Outlet impeller diameter	ε_p	Roughness of different components
η_M	Efficiency at the BEP		
ν_M	Kinematic viscosity		
ε_M	Roughness of different components		

Table 1: Required model and prototype characteristic for the application of the numerical model.

From a list of 57 PATs available in the literature [12], two geometrically resembling pumps were selected based on the dimensionless specific speed. One of them represents the model, while the other describes a pump with a geometry, not similar, but resembling to the prototype's geometry, 1.

This resembling prototype "rp" not only is con-

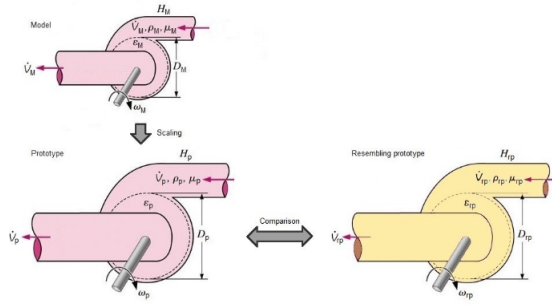


Figure 1: Scheme of the numerical model

sidered as the reference to evaluate the dispersion of the estimated values, but also as the element required to determine the prototype's initial characteristics. In order to evaluate the proximity between the prototype and the resembling prototype, some characteristics of the former must be stipulated as equal to the corresponding characteristics of the latter. In this way, the optimum power and rotational speed of the prototype are assumed as equal to those of the resembling prototype. With both the power and rotational speed of the prototype, the remaining operating characteristics are calculated by means of the model characteristics and the similarity laws enunciated previously. The similarity laws also state that the efficiency of the model is equal to the efficiency of the prototype.

The presence of the Reynolds number and roughness on a pump is frequently neglected. However, it can be of significant influence. Apart from the mechanical losses, which are assumed to be constant both for the model and prototype, the remaining losses are Reynolds and roughness dependent. As such, there are some factors that are used to correct the characteristics of the prototype that were once estimated through the similarity laws: efficiency correction factor f_η ; flow rate correction factor f_Q ; and head correction factor f_H . These correction factors represent the influence that the Reynolds number and roughness have on the PAT operating characteristics. Detailed information regarding the calculation of these factors is found in [7].

The losses discussed in the previous section 4 are important to consider the efficiency of the PAT. All of them can be calculated through more or less extensive equations, see [7] detailed information. With each specific loss identified, the efficiency correction factor can be determined. As a consequence, the performance correction factors that represent the influence of the roughness and Reynolds number are finally characterized. These factors, when multiplied by the PAT corresponding characteristics, result in the new performance values that take into account the roughness and

Reynolds number variants for a scaled version of the model, Eqs. 6 to 9 .

$$\eta_B = \eta_A \cdot f_\eta \quad (6)$$

$$\frac{Q_B}{Q_A} = \frac{N_B}{N_A} \left(\frac{D_{2B}}{D_{2A}} \right)^3 \cdot f_Q \quad (7)$$

$$\frac{H_B}{H_A} = \left(\frac{N_B}{N_A} \right)^2 \left(\frac{D_{2B}}{D_{2A}} \right)^2 \cdot f_H \quad (8)$$

$$\frac{P_B}{P_A} = \frac{\rho_B}{\rho_A} \left(\frac{D_{2B}}{D_{2A}} \right) \left(\frac{N_B}{N_A} \right)^3 \cdot f_\eta \quad (9)$$

One of the initial considerations stipulated upon the implementation of this procedure states the following: the model and prototype are undoubtedly geometrically similar. Recalling geometrical similarity, two pumps with similar geometry have the same dimensionless characteristics and so, the same specific speed. Therefore, the specific speed of the prototype must be equal to the specific speed of the model. However, the new characteristic values of the PAT comprehend an error associated with the dimensionless specific speed: this parameter, when estimated with the new characteristics of the PAT, differs from the specific speed of the model. Such result leads to the conclusion that some assumption is misleading the calculation of the performance correction factors.

The presence of the efficiency correction factor in the power affinity law (Eq. 9, states that one of its terms must change in order to maintain the prototype's power.

At the beginning of this numerical method, the power and rotational speed of the prototype were defined as constraint variables, meaning, the result of the calculations that follow them depends on the value that these parameters assume. They cannot be modified in the process as they are considered as certain. In addition, any parameter that characterizes the model cannot vary as well, the model and prototype densities must be equal and their number of stages must be the same so that the geometric similarity condition holds true. Therefore, the only variable that can compensate the variation imposed by the efficiency factor is the impeller diameter of the prototype. This means that, after the acquisition of the PAT operating characteristics, a correction of the impeller diameter still has to be taken into consideration. Afterwards, it is mandatory to evaluate the difference between the impeller diameter estimated initially and the corrected impeller diameter in order to verify if the geometric similarity condition remains valid.

5.2. SPATEC – Efficiency Curves Scaling Program

The Scaling of PAT Efficiency Curves program or SPATEC is the Microsoft Excel implementation

of the numerical methodology presented in chapter 5. This program has a database of 57 PATs, from which 35 are reverse-running centrifugal pumps.

The numerical methodology developed in this work relies on a PAT model to calculate the system characteristics of a geometrically scaled prototype. Subsequently, it uses a third PAT (previously defined as resembling prototype) that has a geometry quite similar to the model and prototype to compare the estimated results.

To understand which PATs have the most similar geometries, the dimensions of both machines must be scaled with similar ratios. Such relation between the prototype and the resembling prototype cannot be verified entirely once literature lacks information regarding pump geometries. Therefore, it is assumed in this work as a first approximation that, PATs with close specific speeds imply resembling geometries. Naturally, this condition is not necessarily true. However, at the end of the numerical model the deviation between both the prototype and resembling prototype diameters is calculated and its modulus evaluated.

As a result of this geometry assumption, the 57 PATs were re-organized by specific speed to understand which PATs come closer to each other geometrically. Afterwards, each PAT was considered as the model and possible resembling prototypes were selected according to the following condition: the specific speed deviation between the prototype and the resembling prototype should be lower or equal to 0.05, i.e $\Delta\Omega < 0.05$. From this criterion it was obtained 95 cases that relate different PATs.

The specific speed deviation condition is necessary in the screening process but not sufficient. In addition to this restriction, the cases must also be analyzed with respect to their geometric category, which is provided in each PAT formulae. If one of the previous cases combines two PATs with distinct geometries, then it shall be removed from the test data.

The prediction of the prototype's efficiency curve depends on the diameter of the model. Whenever this parameter is unknown for both PATs, the estimation of the efficiency curve is not possible and the respective case must be excluded as well.

Finally, for the last restriction it is stipulated that the rotational speed of the resembling prototype must be constant for the points of operation used in the analysis. These points must have the same rotational speed so that, when compared to the prototype points of operation, both efficiency curves fall over the same coordinate plane. This restriction could be avoided by using similarity laws to transform the different points of operation into the same plane of rotational speed. However, in this thesis, it was decided not to apply this procedure

so that the experimental results (resembling prototype points of operation) would not be subject to additional errors.

The numerical model used to predict PAT efficiency curves was developed with the aid of Microsoft Excel. The program is divided into four sections: Reynolds and roughness correction; specific speed correction; diameter correction - iterative process; and PAT performance.

At the first stage, the program requires the input of the best efficiency point operating characteristics of both the model and resembling prototype. With such data, the numerical calculations result in the initial correction factors. At the subsequent stage, the former factors and the impeller diameter are corrected as a consequence of the specific speed correction.

The parameters determined in the two first sections are used in the third stage to evaluate the deviation between the estimated and the corrected diameter ΔD_{2p} and, subsequently, the worthiness of the next iteration: if $\Delta D_{2p} \leq 1$ mm, then the iterative process stops; otherwise, the initially estimated diameter shall be replaced by the corrected diameter. In this way, the calculations associated with the first and second stages are repeated, and the resulting correction factors are attained with a higher precision. Three iterations are applied for each case. The PAT performance stage reproduces the prototype operating points. Such points are achieved through the application of the correction factors and the affinity laws to the various operating points of the model.

At the end of the program, the model, prototype and resembling prototype efficiency curves are represented graphically as a function of the flow rate and, subsequently, as a function of the PAT's head. These graphics allow to understand the variation between the model and the prototype and to evaluate the closeness of the prototype and resembling prototype curves, as shown in Fig. 2

6. Analysis and Discussion of Results

From the 40 cases that were selected to test the numerical model, some predicted quite successfully the prototype efficiency curves. However, there were other cases that fall short on what was verified experimentally with their respective resembling prototypes. A lower, an intermediate and an upper specific speed group were assumed as the best way to divide all cases, see fig. 3 to perceive the group division delimited by the black intermittent lines.

Whilst these case groups have specific speeds varying between 0.12 and 0.89 it does not mean that it is not possible to apply the numerical model to a PAT with a higher or lower specific speed. One of the problems faced when developing this theory

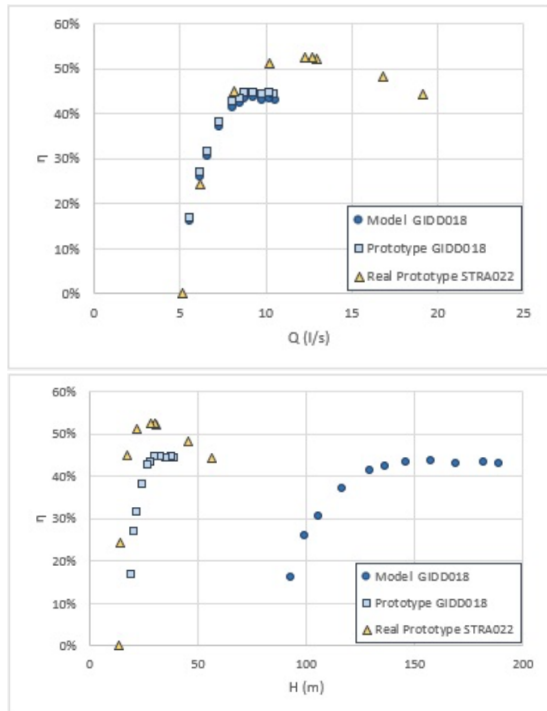


Figure 2: Efficiency curves as a function of the flow rate and the head

is that it is impossible to know whether resembling prototypes have the same geometry as the prototypes to which they were correlated. Due to the lack of information regarding the geometry of the PATs and, in order to proceed with the efficiency prediction study, it was assumed that equal specific speeds imply equal geometries. However, as explained above, it is evident that if the prototype diameter differs considerably from the resembling prototype diameter, then the PATs have different geometries and, therefore, the similar geometry is infringed and there is a larger error associated with the efficiency prediction.

Viewed as one of the most important variables in this work, the specific speed allows not only to represent the geometry of a PAT family, but also to evaluate the accuracy of the PAT efficiency prediction. This accuracy naturally depends on the deviation between the specific speed of the prototype and resembling prototype.

One of the outputs of the numerical model characterizes the prototype diameter. This parameter, together with the resembling prototype diameter represents a crucial feature of the case to be analyzed. Through these two variables it is possible to draw conclusions about the geometric proximity, assumed to be similar for the comparison of efficiency curves. Therefore, to understand how diameters differ across the 40 cases it is necessary to estimate the respective absolute ΔD_{abs} and relative ΔD_{rel} errors. The first represents the metric difference between the prototype and the re-

sembling prototype diameters. The second characterizes the percentage difference that the prototype diameter presents compared to the resembling prototype diameter.

If the relative error is greater than 10%, then the similar geometry condition is automatically refuted, and the error associated with the efficiency prediction higher. Otherwise (i.e. $\leq 10\%$), the geometric relationship between the prototype and the resembling prototype is maintained as similar and the error associated with efficiency prediction lower.

It is clear that, from the 40 cases to which the numerical model has been applied, there is a high number of cases that do not illustrate the diameter difference, as observed in Fig. 3.

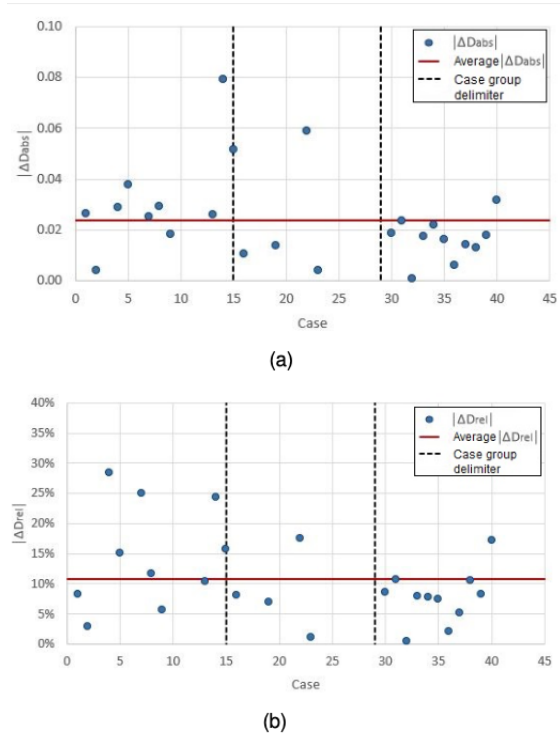


Figure 3: (a) Diameter absolute error, (b) Diameter relative error

In an overall point of view 72% of the cases (excluding the invalid cases) exhibit approximately an impeller diameter difference lower or equal to 10%, which is assumed as a satisfying result.

To compare the efficiency curves between the prototype and the resembling prototype it is necessary to determine the efficiencies of the prototype that correspond to the diverse flow rates and heads of the resembling prototype. This alignment allows the calculation of the absolute and relative errors associated with each operating point. A linear regression is then the most appropriate method to estimate the efficiencies.

By replacing the flow rates and heads of the resembling prototype on the prototype trendline, it is determined the absolute and relative error as-

sociated with the numerical method developed in this work. After some restriction rules are established, the absolute and relative errors associated with the prototype efficiency prediction are evaluated, as seen in Fig. 4. If any resembling prototype point of operation is out of the operating range of the prototype, the error calculation should be estimated via an extrapolation method.

H(m)	η_{rp}	η_{TL}	$\Delta\eta_{abs}$	$\Delta\eta_{rel}$	Δe_{abs}	Δe_{rel}
56.24	44.4%	-108.7%	-153.1%	-344.7%	329.8%	-2203.9%
45.30	48.3%	33.8%	-14.5%	-30.0%	6.7%	-86.0%
30.73	52.1%	44.3%	-7.8%	-15.0%		
30.13	52.4%	44.2%	-8.2%	-15.7%		
28.38	52.4%	43.6%	-8.8%	-16.7%		
22.01	51.0%	32.6%	-18.4%	-36.1%		
17.32	44.9%	1.3%	-43.6%	-97.0%	61.0%	-169.0%
14.23	24.4%	-40.3%	-64.7%	-265.2%	229.2%	-635.2%
13.21	0.0%	-59.2%	-59.2%	#DIV/0!	#DIV/0!	#DIV/0!

(b)

Q(l/s)	η_{rp}	η_{TL}	$\Delta\eta_{abs}$	$\Delta\eta_{rel}$	Δe_{abs}	Δe_{rel}
19.11	44.4%	-134.4%	-178.8%	-402.8%	172.1%	-2545.4%
16.78	48.3%	-58.4%	-106.7%	-221.0%	100.0%	-1479.0%
12.98	52.1%	21.1%	-31.0%	-59.5%	24.3%	-358.9%
12.71	52.4%	24.6%	-27.8%	-53.0%	21.0%	-310.8%
12.30	52.4%	29.5%	-22.9%	-43.7%	16.1%	-238.8%
10.24	51.0%	44.2%	-6.8%	-13.25%		
8.18	44.9%	42.8%	-2.1%	-4.68%		
6.15	24.4%	25.6%	1.2%	4.72%		
5.12	0.0%	10.8%	10.8%	#DIV/0!	9.6%	837.2%

(a)

Figure 4: (a) Flow rate efficiency curve errors, (b) Head efficiency curve errors

In order to understand the impact that each error has, it is selected for all cases the minimum and maximum errors verified amongst all operating points and its values plotted in the same graphic. Taking into account that there are absolute and relative errors for both the head and flow rate efficiency curves, four graphics must be plotted to represent the different characteristic errors, Fig. 5. To analyze the obtained results, the 40 cases are divided into distinct groups according to their specific speed.. For each case, it is assumed that both the range length and its minimum (or initial) value can have high or low values Table 2.

Qualifier	Range Length	Initial Error Value
Small-Small	$\leq 10\%$	$\leq 10\%$
Small-Large	$\leq 10\%$	$> 10\%$
Large-Small	$> 10\%$	$\leq 10\%$
Large-Large	$> 10\%$	$> 10\%$

Table 2: Qualifier description according to range length and minimum error value

Depending on the type of error being analyzed (i.e. absolute or relative error), each qualifier has a particular meaning. Without going into a much detailed explanation, it is important to acknowledge

that, in a general point of view, absolute errors vary approximately between 5% and 20%. As a consequence, it is expected that both the flow rate and head prototype efficiency curves exhibit different shapes when compared to the resembling prototype curves, but at least present an area where the efficiency prediction is carried out with success. As for the relative errors, although their average range differs considerably (8%-50% compared to 8%-140% for flow rate and head curves, respectively), they represent the same meaning in the prediction of efficiencies. Their Large-Small qualifier implies that the prediction uncertainty might be low or high compared to the real efficiency value.

In most cases, the behavior of relative error as a function of flow is expressed by the Large-Small qualifier, meaning, the numerical model estimates the prototype efficiencies with both low and high uncertainties.

The errors calculated demonstrate a numerical model that is associated not only with a high relative error, but also an absolute. Such errors have often been justified on the premise that operating points in the linear zone induce quite significant errors. In order to show that these operating points actually have a high impact on the overall error ranges, it was analyzed the different errors for flow rates and heads that are 10% greater or smaller than the BEP operating characteristics. Although Fig.6 clearly imparts that the length of each error range diminished significantly, it is essential to understand carefully what happened to each error range so that a general outcome of the results can be formulated.

		$e_{min} \uparrow$	$e_{max} \downarrow$	$e_{min} \uparrow \& e_{max} \downarrow$	Both const.	Total
Flow rate	$\Delta\eta_{abs}$	8.3%	41.7%	47.2%	2.7%	100%
	$\Delta\eta_{rel}$	8.3%	47.2%	44.5%	0%	100%
Head	$\Delta\eta_{abs}$	4.2%	37.5%	58.3%	0%	100%
	$\Delta\eta_{rel}$	0%	37.5%	62.5%	0%	100%

Table 3: Relative frequency of range variation

By analyzing Table 3, it is verified that in most cases the total error range either reduces its maximum error and withholds its minimum error, or increases its minimum error and reduces its maximum error. It is only a few percentage of the cases that increase the minimum error and keep the maximum error constant. Apart from the 27th case of the flow rate efficiency curve, that remains with the same error range length, the range restriction applied to the total operating range truly increases the certainty of the error associated with the efficiency curves.

In addition to the analysis of the errors associated with the efficiency prediction, as to the differences between the specific speeds and diameters of the prototype and resembling prototype, it is also interesting to study the sensitivity of the numerical model when certain parameters of its system

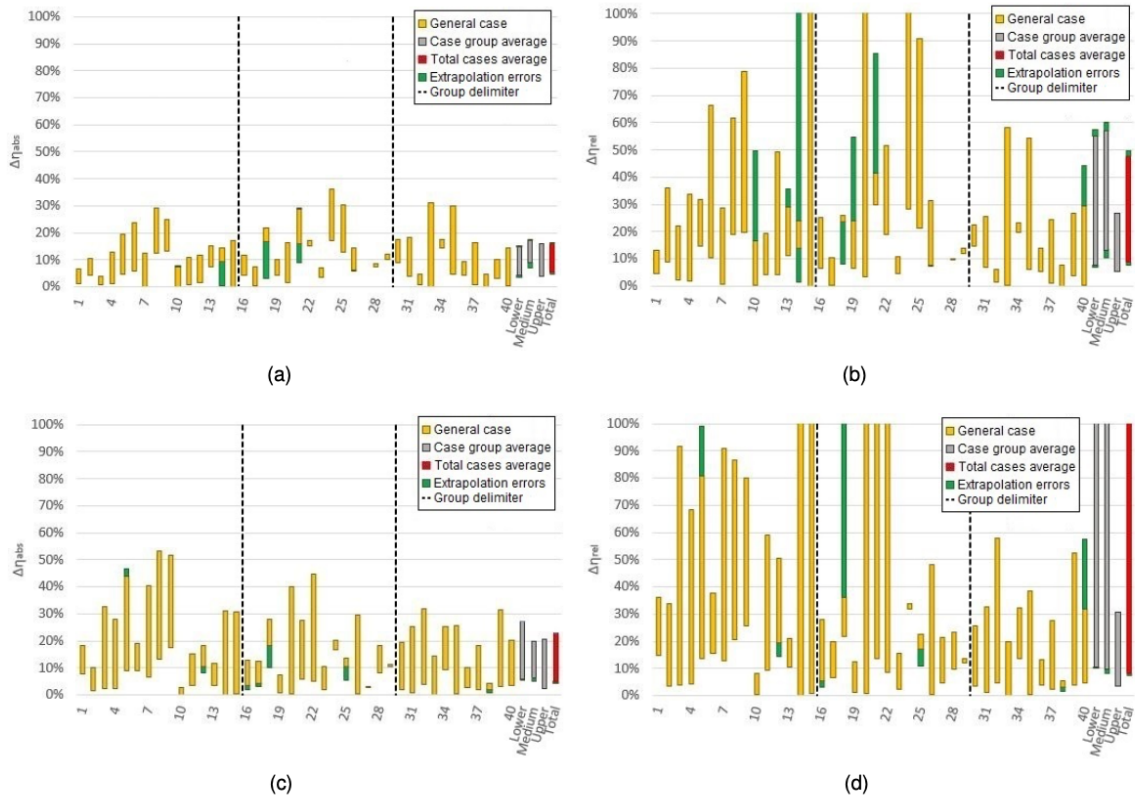


Figure 5: Absolute and relative error ranges for the total operating range of the prototype. (a) flow rate absolute error range, (b) flow rate relative error range, (c) head absolute error range, (d) head relative error range.

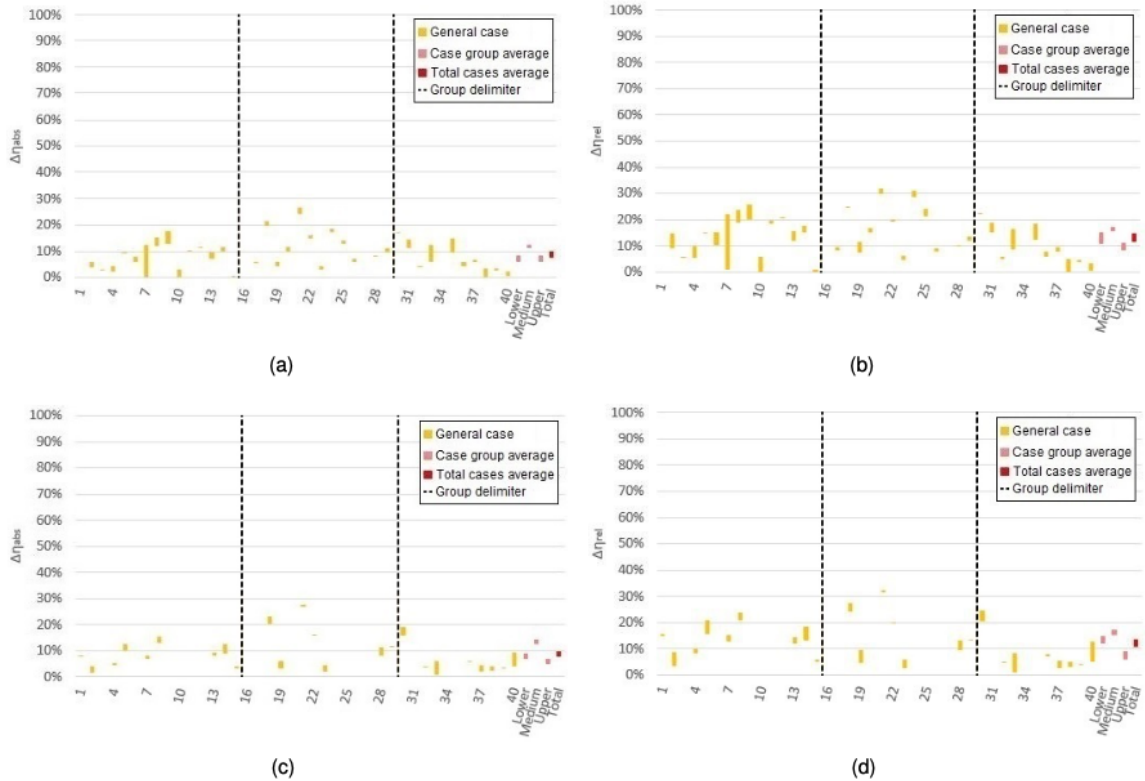


Figure 6: Absolute and relative error ranges for $\pm 10\%$ BEP. (a) flow rate absolute error range, (b) flow rate relative error range, (c) head absolute error range, (d) head relative error range

are subject to variations that are considered significant.

There are several factors that contribute to the efficiency differences between two PATs, most notably the roughness and the Reynolds Number. To understand the impact that these factors have on the efficiency prediction, in each of the 40 cases, it is studied separately the outcome resultant from the variation of $\pm 10\%$ of roughness or kinematic viscosity. To avoid a further extensive analysis of the final results it is feasible to directly compare the correction factors obtained at the end of the numerical model rather than to calculate the new prototype operating points and then compare the efficiency curves, Table 4.

		f_Q	f_H	f_η	D_{2p}
+10% ε	Max	0.22%	0.14%	0.22%	0.10%
	Avg	0.04%	0.03%	0.05%	0.00%
	Min	0.00%	0.00%	0.00%	0.00%
-10% ε	Max	0.20%	0.13%	0.23%	0.01%
	Avg	0.05%	0.03%	0.05%	0.00%
	Min	0.00%	0.00%	0.00%	0.00%
+10% ν	Max	0.25%	0.18%	0.21%	0.01%
	Avg	0.05%	0.03%	0.04%	0.00%
	Min	0.00%	0.00%	0.00%	0.00%
-10% ν	Max	0.26%	0.18%	0.22%	0.10%
	Avg	0.05%	0.03%	0.05%	0.00%
	Min	0.00%	0.00%	0.00%	0.00%

Table 4: Percentage variation of the correction factors and impeller diameter

From an overall point of view, an average variation of approximately 0.05% for each corrective factors is intuitively insignificant. As for the prototype geometry, it is noticeable that the variation of these parameters does not affect the final diameter of the prototype at all.

7. Application of the numerical model to real-life micro hydropower plants

One of the main objectives of this work is to enable the *a priori* study of the economic viability of a micro hydropower system based on the use of a pump working as a turbine for power generation. To do so, it is essential to understand how the numerical model behaves when applied to such systems. In this thesis, it was analyzed the application of the SPATEC program to two systems: Waterval's micro hydropower system with 13kW located in Western Cape, South Africa; and Teutberg's micro hydropower system of 117kW located on the South Coast of South Africa in the Roman Bay Sea Farm. Then, it was compared the theoretical and experimental results of the PATs efficiencies.

For the first case, the prediction presents an extremely high level of success once the absolute and relative errors for both the flow rate and head efficiency curves are satisfyingly below the error ranges established for PAT efficiency prediction. As for the prototype diameter, it was also obtained a reasonable result. For the second case, the efficiency prediction does not exhibit the same quality

as the first, which was expectable since the specific speed deviation between the prototype and the resembling prototype overcomes the acceptable limit of 0.05. Although it was verified a significant absolute error, its importance loses value when associated with a moderately satisfactory relative error. The estimated prototype diameter has a relatively high absolute deviation, which indicates that the geometry of the resembling prototype does not match successfully Teuteberg's PAT geometry.

8. Conclusions

In order to reflect about any problems that may exist in the application of the numerical model, it should be noted the possibility of the geometric similarity condition being invalid and what implications this has in the prediction of efficiencies. Recall the assumption that pumps with equal dimensionless coefficients have similar geometries.

In this work, there were cases with similar and dissimilar diameters. Taking into account that the latest are associated with higher errors, it is up to the user to decide whether or not these errors are acceptable, for example, in the preliminary economic study of an hydropower system.

When it comes to the extrapolation methodology developed in this work, it is brought to a conclusion that, despite having positive influence in the error ranges estimation, the payback fall short when compared to the amount of work invested in the extrapolating process.

In addition to the evaluation of the precision of the numerical model along both efficiency curves, it was also possible to draw conclusions regarding their behavior within a specific operating range, more precisely $\pm 10\%$ BEP. It is now known that to the reduction of the operation range corresponds an almost certain reduction of the maximum error (95%). Likewise, it is concluded that the minimum error is likely to increase or remain constant (55% and 41% respectively). Such results allow not only to realize that the error associated with the efficiency prediction improves, but also that the certainty inherent to the error increases and thus, the results naturally become more reliable.

Although the sample of real cases is reduced, it can be concluded that the prediction of the BEP efficiency was successfully carried out. In one case, the efficiency was predicted with a very satisfying precision, only diverging about 1.5% in both efficiency curves. In the other case, the efficiency deviated a little further from the experimental value (11% in both efficiency curves as well), but still managed to reach a satisfying result.

In addition, as it was intended to prove, it is now possible to conclude that the specific speed has a significant impact on the efficiency curves of a PAT, as it can be seen in fig. 7.

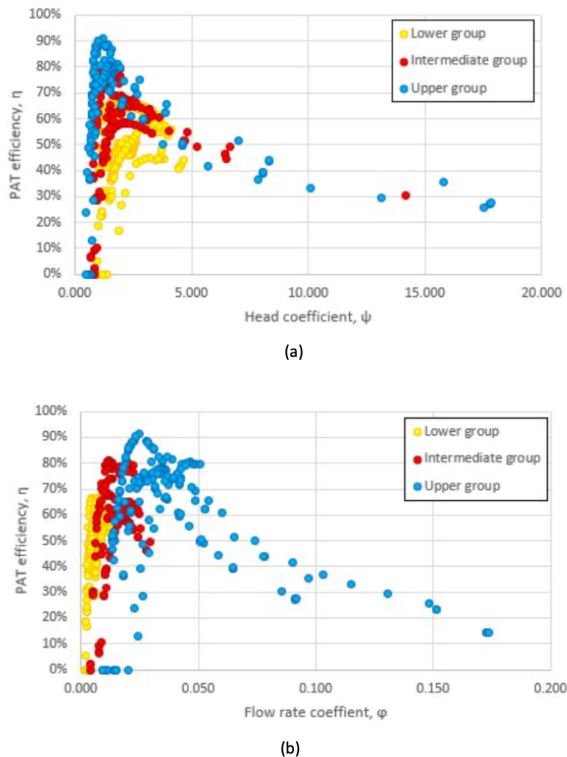


Figure 7: Specific speed influence on the PAT efficiency (a) PAT efficiency as a function of the flow rate coefficient ϕ , (b) PAT efficiency as a function of the head coefficient ψ .

That said, it is concluded that the SPATEC program satisfactorily forecasts the flow rate and head efficiency curves for pumps operating as turbines.

References

- [1] I. H. Association, I. C. on Large Dams, I. A. on Hydropower Technologies, P. E. Agency, and C. H. Association. Hydropower and the world's energy future, November 2000.
- [2] A. Carravetta, G. D. Giudice, O. Fecarotta, and H. M. Ramos. Pat design strategy for energy recovery in water distribution networks by electrical regulation. *Energies*, 6(1):411–424, January 2013.
- [3] A. Carravetta, G. D. Giudice, O. Fecarotta, and H. M. Ramos. Pump as turbine (pat) design in water distribution network by system effectiveness. *Water*, 5(3):1211–1225, August 2013.
- [4] A. Engeda and M. Rautenberg. Comparisons of the performance of hydraulic turbines and reversible pumps for small-hydro applications. 5th International Symposium on Hydro Power Fluid Machinery, 1988. FED -68.
- [5] A. F. O. Falcão. *Mecânica dos Fluidos II*. 1st edition, 2015.
- [6] Fraser and Associates. Modular small hydro configuration. Report Nyserda, 1981. 81-16.
- [7] J. F. Gülich. *Centrifugal Pumps*. Springer, 2nd edition, 2010. Chapters 1-3.
- [8] P. Hergt, P. Krieger, and S. Thommes. Die strömungstechnischen eigenschaften von kreiselpumpen im turbinenbetrieb. Pumpentagung Karlsruhe, 1984. Section C1.
- [9] F. Hochreitiner. Centrale hydroélectrique de tannuwald. Hydroenergia 1991 Conference Proceedings, 2nd International Conference Exhibition, 1991.
- [10] A. A. Inc. Small hydroplant development program, 1980.
- [11] A. Kumar and O. Thapar. Integrated small hydro energy development. Conference "Water for Resource Development", 1984.
- [12] I. S. Paterson and C. S. Martin. Effect of specific speed on pump characteristics and hydraulic transients in abnormal zones of operation. 12th Symposium of the SHMEC "Hydraulic Machinery in the Energy Related Industries", 1984. 151-72.
- [13] E. Schmiedl. Serien-kreiselpumpen im turbinenbetrieb. Pumpentagung Karlsruhe '88, 1988. Section A6.
- [14] A. J. Semple and W. Wong. The application of hydraulic power recovery turbines in process plant. Second European Congress on Fluid Machinery for the Oil, Petrochemical and Related Industries (The Hague), 1984. C35.227-34.
- [15] G. Ventrone and G. Navarro. Utilizzazione dell'energia idrica su piccola scala: pompa come turbina. *L'Energia Elettrica*, 1982.
- [16] W. Wong. The application of centrifugal pumps for power generation. 10th International Conference of the BPMA, 1987.